

Benzyl Complexes of the Heavier Alkaline-Earth Metals: The First Crystal Structure of a Dibenzylstrontium Complex

Florian Feil and Sjoerd Harder*

Universität Konstanz, Postfach 5560, M738, 78457 Konstanz, Germany

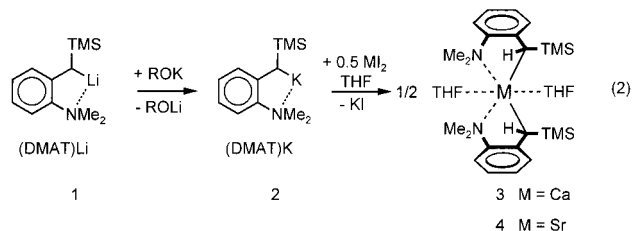
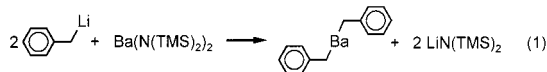
Received May 25, 2001

The first benzylstrontium complex, di(2-Me₂N- α -Me₃Si-benzyl)strontium, has been prepared via reaction of the benzylpotassium complex with SrI₂. The crystal structure of the bis(THF)-solvate complex shows hexacoordination at Sr. Structural analyses and NMR analyses of the related Li, K, and Ca complexes reveal that the delocalization of the negative charge in the phenyl ring is metal dependent and decreases along the row K > Li \geq Sr > Ca. The presented benzylstrontium complex contains two chiral benzylic centers and forms diastereomers. In apolar solvents at room temperature both diastereomers are observed. Either higher temperatures or extra added THF ligands result in fast inversion of the chiral benzylic carbanion. The process is concentration independent and follows a dissociative mechanism in which one of the Sr–C _{α} bonds is broken. The chiral benzylic carbon atom in the strontium complex shows faster inversion than that in the analogue benzylcalcium complex (Ca, 0.07 M, $\Delta G^\ddagger(60^\circ\text{C}) = 16.8 \text{ kcal mol}^{-1}$; Sr, 0.08 M, $\Delta G^\ddagger(30^\circ\text{C}) = 15.0 \text{ kcal mol}^{-1}$). The new benzylstrontium complex is an active initiator for the anionic living polymerization of styrene and is more reactive than its Ca analogue.

Introduction

The syntheses of non-cyclopentadienyl complexes of the heavier alkaline-earth metals (Ca, Sr, Ba) have attracted increasing attention.¹ Most of these complexes contain relatively stable carbanions, facilitating their isolation and handling. The more reactive and nucleophilic alkyl and benzyl complexes received hitherto considerably less attention. Highly polar alkaline-earth benzyls, which are potent initiators for the polymerization of styrene, were usually prepared in small quantities via undesirable synthetic procedures (reaction of alkaline-earth metal mirrors with dibenzylmercury).² The products are generally obtained in situ and not very well characterized. We recently published an easy preparative procedure for dibenzylbarium (eq 1),³ but were not able to obtain the compound in crystalline purity. Similar synthetic strategies for the Ca or Sr analogues failed due to incomplete exchange.⁴ However,

a well-defined crystalline benzylcalcium complex (**3**, (DMAT)₂Ca·(THF)₂)^{5a} could be prepared in good yields via a ligand metathesis reaction (eq 2).^{5b} The TMS and Me₂N substituents increase bulk and donor properties of the benzyl ligand and facilitate the synthesis by increasing stability and solubility of the calcium compound (good solubility is a prerequisite for product/KI separation). Unfortunately, these substituents simultaneously retard the initiation step for the anionic polymerization of styrene. The earlier reported benzylcalcium complex (**3**) can nevertheless be used in the anionic polymerization of styrene. However, the initiation step is slow: GPC spectra of the obtained polystyrene show a tailing in the low molecular weight range.



(1) (a) Cloke, F. G. N.; Hitchcock, P. B.; Lappert, M. F.; Lawless, G. A.; Royo, B. *J. Chem. Soc., Chem. Commun.* **1991**, 724. (b) Mashima, K.; Sugiyama, H.; Kamehisa, N.; Kai, Y.; Yasuda, H.; Nakamura, A. *J. Am. Chem. Soc.* **1994**, *116*, 6977. (c) Overby, J. S.; Hanusa, T. P. *Angew. Chem.* **1994**, *106*, 2300; *Angew. Chem., Int. Ed. Engl.* **1994**, *33*, 2191. (d) Eaborn, C.; Hawkes, S. A.; Hitchcock, P. B.; Smith, J. D. *J. Chem. Soc., Chem. Commun.* **1997**, 1961. (e) Harder, S.; Lutz, M. *Organometallics* **1997**, *16*, 225. (f) Harvey, M. J.; Hanusa, T. P.; Young, V. G., Jr. *Angew. Chem.* **1999**, *111*, 241; *Angew. Chem., Int. Ed.* **1999**, *38*, 217. (g) Westerhausen, M.; Digeser, M. H.; Gückel, C.; Nöth, H.; Knizek, J.; Ponikvar, W. *Organometallics* **1999**, *18*, 2491. (h) Green, D. C.; English, U.; Ruhlandt-Senge, K. *Angew. Chem.* **1999**, *111*, 365; *Angew. Chem., Int. Ed.* **1999**, *38*, 354.

(2) (a) West, P.; Woodville, M. C. United States Patent 3,718,703, 1973. (b) Paleeva, I. E.; Sheverdina, N. I.; Kocheshkov, K. A. *J. Gen. Chem. USSR* **1974**, *44*, 1091. (c) De Groof, B.; Van Beylen, M.; Szwarc, M. *Macromolecules* **1975**, *8*, 396.

(3) Weeber, A.; Harder, S.; Brintzinger, H.-H.; Knoll, K. *Organometallics* **2000**, *19*, 1325.

(4) Harder, S.; Weeber, A. Unpublished results.

We here present an easy synthesis for a well-defined crystalline dibenzylstrontium complex: di(2-Me₂N- α -Me₃Si-benzyl)strontium ((DMAT)₂Sr·(THF)₂; **4**), the

(5) (a) DMAT is an abbreviation for 2-dimethylamino- α -trimethylsilylbenzyl. (b) Harder, S.; Feil, F.; Weeber, A. *Organometallics* **2001**, *20*, 1044.

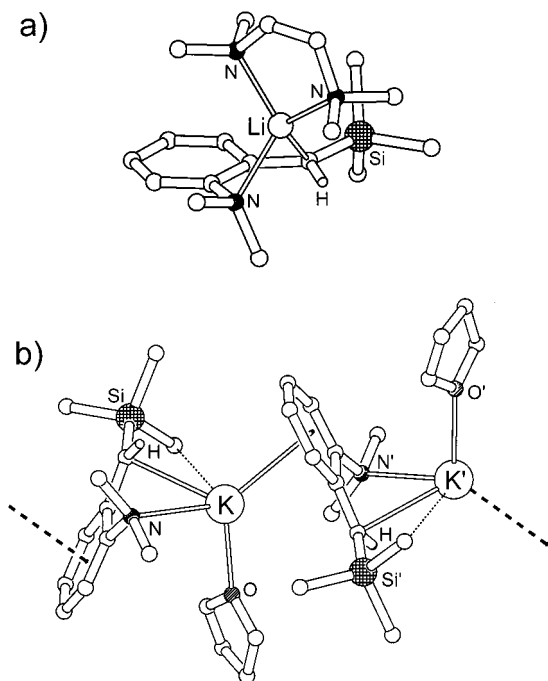


Figure 1. (a) Crystal structure of (DMAT)Li-TMEDA (**1**, only the benzylic hydrogen is shown). (b) Crystal structure of $\{(\text{DMAT})\text{K}\cdot\text{THF}\}_\infty$ (**2**, only the benzylic hydrogen is shown). Agostic $\text{SiMe}\cdots\text{K}^+$ interactions are shown by thin dotted lines (shortest $\text{K}\cdots\text{H}$ and $\text{K}\cdots\text{C}$ distances measure 3.24 and 3.792(4) Å, respectively).

strontium analogue of **3**. Its crystal structure determination reveals the first structural data on a benzylstrontium moiety.

The new strontium complex is, like the previously published Ca analogue (**3**), a diastereomer with two carbanionic centers of opposite chirality. Dynamic NMR studies reveal the first data on the stability of a stereogenic carbanion attached to a Sr^{2+} cation.

The reactivity of the benzylstrontium complex as an initiator for anionic styrene polymerization has been tested and is compared to that of its Ca analogue.

Results and Discussion

Complex **4**, $(\text{DMAT})_2\text{Sr}\cdot(\text{THF})_2$, was prepared in good yield (79%) as a crystalline compound via ligand metathesis between SrI_2 and $(\text{DMAT})\text{K}$ (eq 2). The structures of the precursory benzylmetal complexes, $(\text{DMAT})\text{Li}$ (**1**) and $(\text{DMAT})\text{K}$ (**2**), have also been determined. This enables the comparison of a range of crystal structures in which the DMAT anion is attached to four different metal cations: Li^+ , K^+ , Ca^{2+} , or Sr^{2+} .

The crystal structures of the alkali metal compounds are shown in Figure 1 (selected bond distances and angles are presented in Scheme 1). The TMEDA-solvated Li compound $(\text{DMAT})\text{Li}\cdot\text{TMEDA}$, **1** shows a monomeric structure that is common for benzyl lithium complexes in the presence of Lewis bases.⁶ The benzyl lithium complex is closely related to 2- Ph_2P -

$\alpha\text{-Me}_3\text{Si}$ -benzyl lithium-TMEDA^{6c} and shows a remarkable structural similarity. The analogue potassium compound (**2**), however, displays a completely different structure: it crystallizes as a polymeric chain structure in which the aryl rings bridge to the next unit. This tendency for the formation of coordination polymers is due to the larger coordination sphere of K^+ and its strong preference for binding delocalized π -ligands. This is also observed in the few other known benzylpotassium structures: $[\text{PhCH}_2\text{K}\cdot\text{PMDTA}]_\infty$,⁷ $[\text{PhCH}_2\text{K}\cdot\text{THF}]_\infty$,⁸ and $[\text{Ph}(\text{TMS})_2\text{CK}]_\infty$.⁹ The K^+ cation in $[(\text{DMAT})\text{K}\cdot\text{THF}]_\infty$ is additionally solvated by one THF ligand, and this prevents formation of higher dimensional networks via agostic $\text{SiMe}\cdots\text{K}^+$ interactions, as has been observed in the structure of the Lewis base-free $[\text{Ph}(\text{TMS})_2\text{CK}]_\infty$. The structure of $[(\text{DMAT})\text{K}\cdot\text{THF}]_\infty$ shows only minor agostic interactions within the polymeric chain (Figure 1b). These agostic contacts are much longer than those observed in $[\text{Ph}(\text{TMS})_2\text{CK}]_\infty$.⁹ A comparison of the mono-THF solvates $[\text{PhCH}_2\text{K}\cdot\text{HF}]_\infty$ and $[(\text{DMAT})\text{K}\cdot\text{THF}]_\infty$ shows the influence of introducing large bulky groups (TMS) and intramolecular coordinating substituents (NMe_2). The structure of $[\text{PhCH}_2\text{K}\cdot\text{THF}]_\infty$ forms a complicated more-dimensional network (every K^+ is surrounded by at least three benzyl anions), whereas the network in $[(\text{DMAT})\text{K}\cdot\text{THF}]_\infty$ progresses in only one dimension (each K^+ is bonded to two DMAT anions).

The crystal structures of the alkaline-earth metal compounds are shown in Figure 2 (selected bond distances and angles are presented in Scheme 1). Di(2- Me_2N - $\alpha\text{-Me}_3\text{Si}$ -benzyl)strontium crystallizes from THF/hexane mixtures as the THF-solvate $(\text{DMAT})_2\text{Sr}\cdot(\text{THF})_2$. Its crystal structure and the metal/THF ratio are, despite the somewhat larger coordination sphere for Sr^{2+} (the ionic radii for Ca^{2+} and Sr^{2+} are 0.99 and 1.12 Å, respectively), closely related to that of the earlier reported $(\text{DMAT})_2\text{Ca}\cdot(\text{THF})_2$. The asymmetric unit contains a third THF ligand, which fills up holes in the crystal packing and is not coordinated to the metal.¹⁰ Also $(\text{DMAT})_2\text{Sr}\cdot(\text{THF})_2$ crystallizes as a diastereomer in which both (*R* and *S*) configurations for the chiral benzylic carbon are present in the same molecule. Despite the striking similarity between the Ca and Sr complexes, some difference in the metal coordination geometries is observed. The coordination geometry for Ca is a slightly distorted octahedron (trigonal antiprism) with the carbanions in trans position ($\text{C}_\alpha\text{-Ca-C}_{\alpha'}$ 157.5(1)°) and all neutral coordinating groups in one plane. The coordination geometry for Sr, however, is strongly distorted from the octahedron and more resembles a trigonal prism ($\text{C}_\alpha\text{-Sr-C}_{\alpha'}$ 143.5(1)°). Apart from differences in the coordination geometry, also differences in the benzyl-metal interaction are observed: the benzylic ligands purely bind bidentate to Ca via C_α and N, whereas for Sr additional bonding to

(7) Hofmann, D.; Bauer, W.; Hampel, F.; van Eikema Hommes, N. J. R.; Schleyer, P. v. R.; Otto, P.; Pieper, U.; Stalke, D.; Wright, D. S.; Snaith, R. *J. Am. Chem. Soc.* **1994**, *116*, 528.

(8) Westerhausen, M.; Schwarz, W. Z. *Naturforsch.* **1998**, *B53*, 625.

(9) Feil, F.; Harder, S. *Organometallics* **2000**, *19*, 5010.

(10) The extra noncoordinating THF ligand cocrystallizes only from THF/hexane solutions that are rich in THF (ratio \approx 1:1). Solutions with less THF (1:2 or less) yield after cooling crystals without the extra noncoordinating THF ligand. The latter crystals were used for all the NMR and polymerization studies.

(6) (a) Zarges, W.; Marsch, M.; Harms, K.; Boche, G. *Chem. Ber.* **1989**, *122*, 2303. (b) Zarges, W.; Marsch, M.; Harms, K.; Koch, W.; Frenking, G.; Boche, G. *Chem. Ber.* **1991**, *124*, 543. (c) Byrne, L. T.; Engelhardt, L. M.; Jacobsen, G. E.; Leung, W.-P.; Papasergio, R. I.; Raston, C. L.; Skelton, B. W.; Twiss, P.; White, A. H. *J. Chem. Soc., Dalton Trans.* **1989**, 105.

Scheme 1

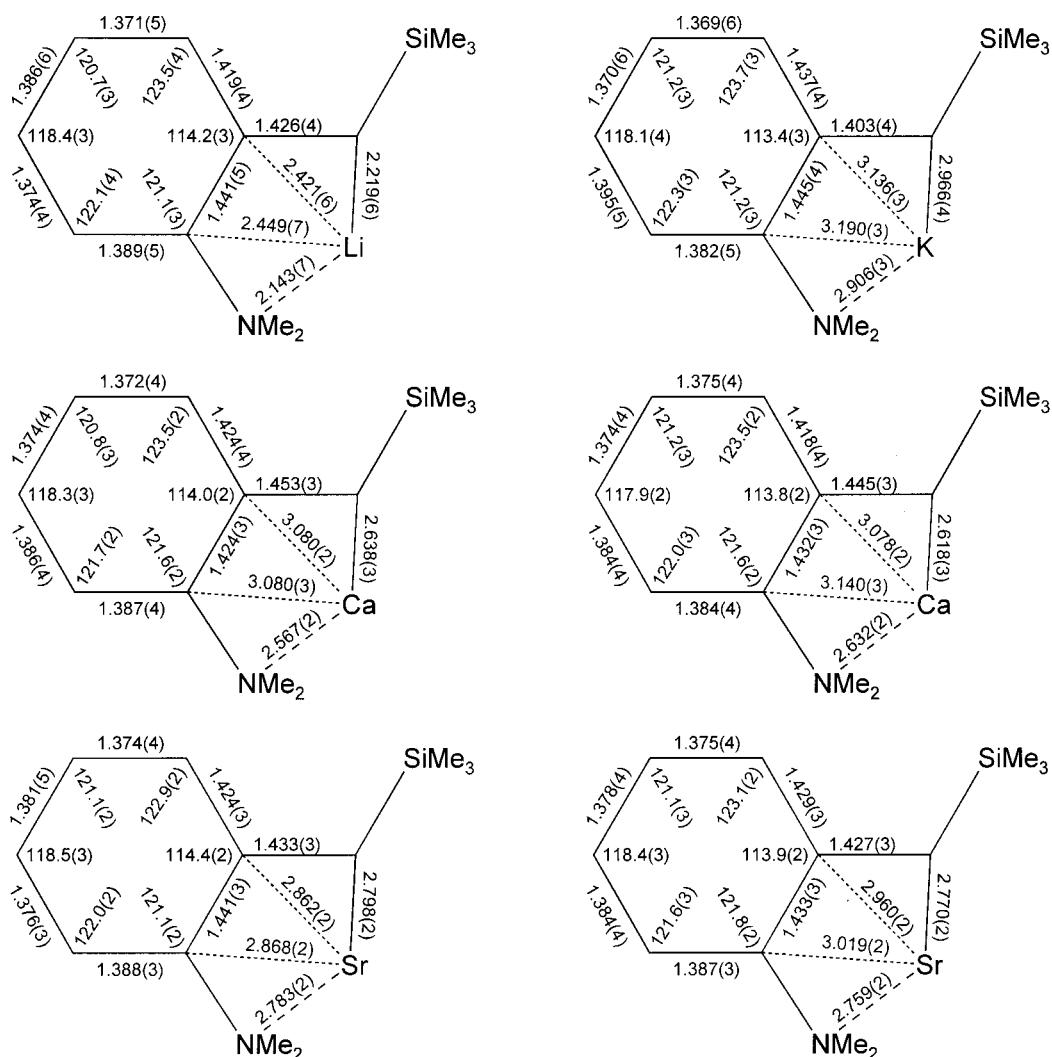


Table 1. Several Characteristic Structural Features and NMR Data for DMAT–Metal Complexes

	$C_{\alpha}-C_{\text{ipso}}$ (Å)	Σ (angles at C_{α}) (deg)	$^1J(C_{\alpha}-H)$ (Hz)	$\delta(^1H_{\text{para}})$ (ppm)	$\delta(^{13}C_{\text{para}})$ (ppm)
(DMAT)Li	1.426(4)	357.96	123.2	6.29	107.0
(DMAT)K	1.403(4)	359.84	131.8	5.78	102.7
(DMAT) ₂ Ca	1.453(3)	342.06	116.0	6.27	112.4
	1.445(3)	345.65	116.8	6.38	112.4
(DMAT) ₂ Sr	1.433(3)	349.51	118.9	6.25	110.7
	1.427(3)	350.70	121.5	6.32	110.8

the aryl ring is observed. Especially, one of the ligands shows short $C_{\text{aryl}}\cdots\text{Sr}$ distances (see Scheme 1). Not many organostrontium complexes are known for a comparison of the Sr–C bond lengths. The average Sr– C_{α} bond distance in **4** (2.781(2) Å) is shorter than the average Sr–C distance in $[(i\text{-Pr})_3\text{Cp}]_2\text{Sr}\cdot\text{THF}$ (2.837(3) Å)¹¹ and longer than the average Sr– C_{sp} bonds in a dialkynylstrontium complex (2.708(4) Å)^{1h} and a Sr-diene complex (2.740(7) Å).^{1b}

Several characteristic structural features and NMR data can serve as a probe to estimate the extent of charge delocalization in a benzyl anion.^{7,9} The availability of structural and spectroscopic data on complexes **1–4** allows an evaluation of the charge delocalization in the DMAT anion as a function of the metal cation.

The most sensitive structural parameters (listed in Table 1) are the $C_{\alpha}-C_{\text{ipso}}$ bond distance and the planarity of the benzylic carbon (expressed as the sum of nonmetal valence angles at C_{α}). Delocalization of the benzylic charge in the aryl ring is counteracted by the localizing influence of the positively charged metal cation. This is a mainly electrostatic effect: a high cation charge and short cation– C_{α} distances lead to a high degree of charge localization. Thus, the general order for charge delocalization is (alkalimetal)–benzyl > (alkaline-earth metal)–benzyl and (large cation)–benzyl > (small cation)–benzyl. The most extensive charge delocalization is observed for the K–benzyl (shortest $C_{\alpha}-C_{\text{ipso}}$ and most planar C_{α}), whereas the Ca–benzyl shows the highest degree of charge localization. The Li–benzyl shows an only slightly larger (nearly similar) degree of charge delocalization than the Sr–benzyl.

(11) Burkey, D. J.; Hanusa, T. P. *Acta Crystallogr.* **1996**, C52, 2452.

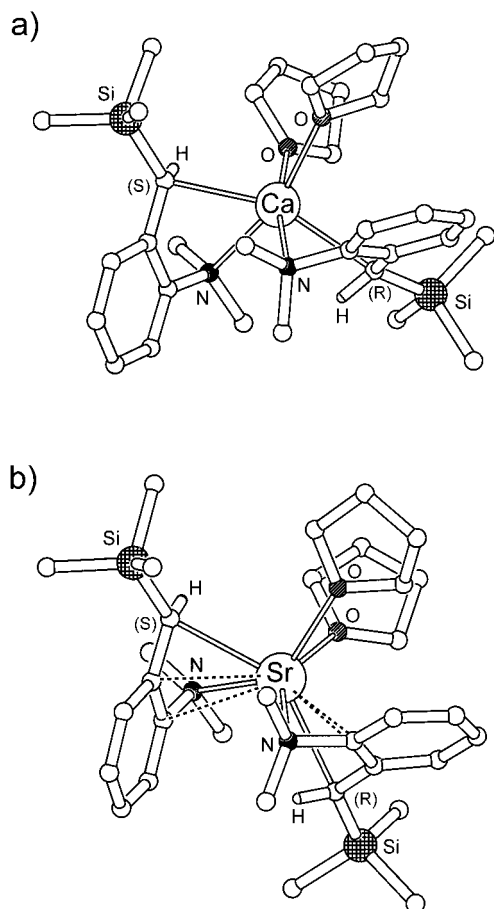
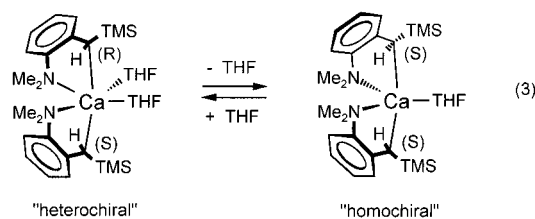


Figure 2. Comparison of the crystal structures of (a) $(\text{DMAT})_2\text{Ca}\cdot(\text{THF})_2$, **3**, and (b) the structure of $(\text{DMAT})_2\text{Sr}\cdot(\text{THF})_2$, **4** (only the benzylic hydrogens are shown). The DMAT ligand acts as a bidentate ligand for Ca, but shows more extensive coordination for Sr (dashed lines represent short distances; see also Scheme 1).

Three important NMR parameter (listed in Table 1) can be used to determine the extent of charge delocalization for benzyl compounds in solution. The $^1J(\text{C}_\alpha\text{--H})$ is very sensitive to the hybridization and therefore the planarity of C_α : large values correlate with planar structures and a high degree of charge delocalization. The chemical shifts for the para-hydrogen and para-carbon are sensitive toward π -electron density and therefore charge delocalization: small chemical shifts indicate high π -charges. The order of charge delocalization found for the metal–benzyls in the solid state ($\text{Ca} < \text{Sr} \leq \text{Li} < \text{K}$) correlates well with that observed in solution. It should be noted that also the colors of the benzylmetal solids and solutions are related to the extent of charge delocalization: stronger delocalization usually leads to more intense coloring and a yellow \rightarrow red shift.

Both alkaline-earth complexes presented here (**3** and **4**) contain two chiral centers and are diastereomers. Inversion of one chiral carbon, commonly observed in sp^3 -carbanionic compounds, results in a diastereomer change (“heterochiral” \leftrightarrow “homochiral”). It should be noted that the chosen DMAT system does not allow free rotation around the $\text{C}_\alpha\text{--C}_{\text{ipso}}$ bond for steric reasons. Therefore, inversion at C_α proceeds via a mechanism in which the metal changes to the other side of the benzyl plane. NMR studies of $(\text{DMAT})_2\text{Ca}\cdot(\text{THF})_2$ and

$(\text{DMAT})_2\text{Sr}\cdot(\text{THF})_2^{10}$ in benzene (or toluene) show at room temperature two sets of signals which can be assigned to their two different diastereomers in slow exchange. For both systems fast exchange is reached by either increasing the temperature or by adding extra THF. The coalescence temperature for the calcium compound is concentration dependent (0.07 M , $\Delta G^\ddagger(T_{\text{coal}} 60\text{ }^\circ\text{C}) = 16.8(3)\text{ kcal mol}^{-1}$; 0.39 M , $\Delta G^\ddagger(T_{\text{coal}} 40\text{ }^\circ\text{C}) = 15.8(2)\text{ kcal mol}^{-1}$), whereas that for the strontium compound shows no dependency on the concentration (0.03 and 0.08 M samples both show the same coalescence temperature: $\Delta G^\ddagger(T_{\text{coal}} 30\text{ }^\circ\text{C}) = 15.0(3)\text{ kcal mol}^{-1}$). Intuitively, one would explain this fundamental difference by proposing an associative exchange mechanism for the Ca compound and a dissociative mechanism for the Sr complex. However, as we pointed out earlier,⁵ there is proof that the “homochiral” diastereomers of $(\text{DMAT})_2\text{Ca}$ (*R, R* and *S, S*) are sterically congested and only contain one THF ligand (eq 3):



(i) The diastereomer ratio for the calcium compound is strongly temperature dependent and shows a considerable negative entropy ($\Delta H^\ddagger = 3.45(7)\text{ kcal mol}^{-1}$ and $\Delta S^\ddagger = -12.1(3)\text{ cal mol}^{-1}\text{ K}^{-1}$).¹²

(ii) The diastereomer ratio for the calcium compound is also strongly dependent on the absolute concentration.

(iii) The chemical shift for the THF ^1H NMR signals, which represents an average value for free and coordinated THF in fast exchange, is also temperature and concentration dependent.

All of these three observations do not hold for the strontium analogue: the diastereomer ratio is temperature and concentration independent ($A/B = 62:38$; estimated $\Delta H^\ddagger = 0.2(2)\text{ kcal mol}^{-1}$ and $\Delta S^\ddagger = 0.2(7)\text{ cal mol}^{-1}\text{ K}^{-1}$), and no temperature dependency for the ^1H NMR THF signals is observed. Obviously, both diastereomers of the strontium complex contain two coordinated THF ligands. The larger ionic radius for Sr^{2+} prevents any steric congestion and loss of THF.

According to the observations listed above, we propose a dissociative mechanism (transition state **5**) for the exchange of the Sr diastereomers. Exchange of the calcium diastereomers also proceeds via a dissociative mechanism; however, the availability of small amounts of free THF (the amount is concentration and temperature dependent) partially assists the exchange reaction via transition state **6**.

Both (alkaline-earth)–benzyls show a higher configurational stability than the alkali metal–benzyls (the latter usually show inversion barriers around 9–12 kcal/mol).¹³ This is partly due to intramolecular chelation,

(12) The values reported in our earlier communication⁵ are wrong and should be multiplied by *R* ($1.9872\text{ cal K}^{-1}\text{ mol}^{-1}$).

(13) (a) Hoffmann, R. W.; Rühl, T.; Chemla, F.; Zahneisen, T. *Liebigs Ann. Chem.* **1992**, 719. (b) Hoffmann, R. W.; Dress, R. P.; Ruhland, T.; Wenzel, A. *Chem. Ber.* **1995**, 128, 861. (c) Fraenkel, G. F.; Duncan, J. H.; Martin, K.; Wang, J. *J. Am. Chem. Soc.* **1999**, 121, 10538.

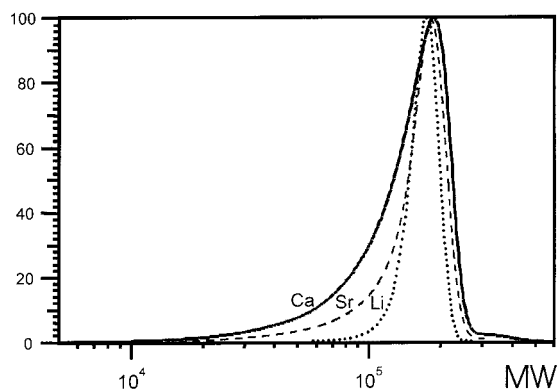
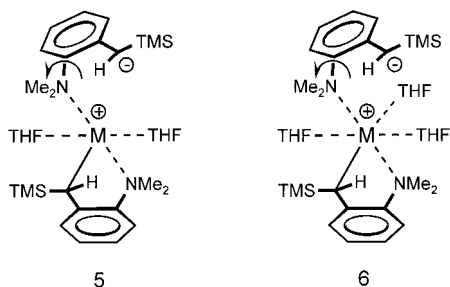


Figure 3. GPCs of polystyrene obtained with a *sec*-BuLi initiator (dotted line, $D = 1.039$), the $(\text{DMAT})_2\text{Sr}\cdot(\text{THF})_2$ initiator (dashed line, $D = 1.218$), and the $(\text{DMAT})_2\text{Ca}\cdot(\text{THF})_2$ initiator (solid line, $D = 1.369$).



which stabilizes chiral carbanions,¹⁴ but also to the stronger bond between the alkaline-earth metal and the carbanion¹⁵ (inversion must involve C–metal bond breaking). Bond weakening down the alkaline-earth group explains the lower configurational stability of the Sr compound compared to its Ca analogue.

The methylamino groups in **3** and **4** are enantiotopic. Consequently low-temperature NMR spectra show four signals arising from the two diastereomers with methylamino groups in slow exchange. The coordinative $\text{Me}_2\text{N}\cdots\text{M}^{2+}$ bond is weaker than the ionic C^--M^{2+} bond. The activation energies for methyl exchange are $(\text{DMAT})_2\text{Ca}\cdot(\text{THF})_2$ 14.5(3) and 15.4(3) kcal/mol; $(\text{DMAT})_2\text{Sr}\cdot(\text{THF})_2$ 13.5(3) and 14.4(3) kcal/mol. It should be noted that the $\text{Me}_2\text{N}\cdots\text{Sr}$ bonds are weaker than the corresponding $\text{Me}_2\text{N}\cdots\text{Ca}$ bonds.

The novel homoleptic alkaline-earth benzyl complexes **3** and **4** are both active initiators for the anionic polymerization of styrene. Polymers obtained with the Ca initiator characteristically show a tailing in the low molecular weight range (Figure 3). Polymers obtained using the more reactive and faster benzylstrontium initiator show significantly less tailing in the lower molecular weight range. However, in comparison with the strongly nucleophilic *sec*-BuLi initiator, still some tailing is observed. This is due to the TMS and NMe_2 substituents, which decrease the nucleophilicity of the initiating DMAT anion. NMR tube polymerizations

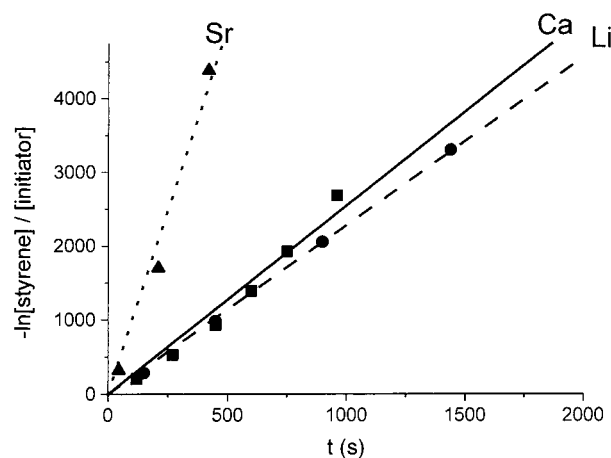


Figure 4. Graphical presentation of $(\ln[\text{styrene}])/[\text{initiator}]$ as a function of the polymerization time (estimated rate constants: Sr $9.94 \text{ L mol}^{-1} \text{ s}^{-1}$, Ca $2.55 \text{ L mol}^{-1} \text{ s}^{-1}$, and Li $2.28 \text{ L mol}^{-1} \text{ s}^{-1}$).

confirm the lethargic behavior of the DMAT anion.¹⁶ This is however only important for the initiation step.

Analyses of chain growth versus time show first-order kinetics with respect to styrene (Figure 4). The reactivity of polystyrylanions is dependent on the counter-cation. The Sr^{2+} counter-cation shows a much higher reactivity than either the Ca^{2+} or Li^+ counter-cations.

The tailing observed in the low molecular weight region of the obtained polymers could also be an indication of nonliving polymerization, i.e., a polymerization with either chain termination or transfer. There is, however, ample evidence that the benzylcalcium and strontium complexes initiate a living polymerization of styrene.

(i) There is a good agreement between observed and calculated molecular weights (usually around 100,000).

(ii) The color of the polymer solution does not change at the end of the reaction and is typical for benzyl anions (orange or red).

(iii) Linear pseudo-first-order kinetic plots are obtained in all cases.

(iv) Stepwise addition of styrene at certain time intervals shows no significant chain termination, and polymers of the final calculated molecular weight are obtained.

(v) The polymerization reactions were followed by NMR:¹⁶ addition of new monomer after a completed polymerization reaction results in renewed polymerization.

(vi) Block polymers with isoprene can be prepared.

Our next goal is the synthesis of stable heteroleptic strontium compounds with a polymerization active benzyl ligand and a nonactive spectator ligand (e.g., Cp) and test such systems for stereoregular polymerization of styrene.

Conclusions

The benzylstrontium complex (**4**) is accessible in good yields through reaction of a benzylpotassium compound

(14) (a) Clark Still, W.; Sreekumar, C. *J. Am. Chem. Soc.* **1980**, *102*, 1201. (b) Strohmman, C.; Abele, B. C.; Schildbach, D.; Strohfeltd, K. *J. Chem. Soc., Chem. Commun.* **2000**, 865.

(15) The C–metal bond strength generally increases on going from the alkali metals to the alkaline earth metals and decreases down the group. This is illustrated by the following calculated energies (MP2/6-31+G* + ZPE) for heterolytic bond dissociation: $\text{PhCH}_2\text{Li} \rightarrow \text{PhCH}_2^- + \text{Li}^+$ (149.3 kcal mol⁻¹); $\text{PhCH}_2\text{Na} \rightarrow \text{PhCH}_2^- + \text{Na}^+$ (127.1 kcal mol⁻¹); $(\text{PhCH}_2)_2\text{BeMe} \rightarrow \text{PhCH}_2^- + \text{MeBe}^+$ (242.4 kcal mol⁻¹); $(\text{PhCH}_2)_2\text{MgMe} \rightarrow \text{PhCH}_2^- + \text{MeMg}^+$ (186.7 kcal mol⁻¹).

(16) NMR experiments showed that a *sec*-BuLi initiator reacts instantaneous with styrene at room temperature (no free styrene could be detected within minutes), whereas the DMAT initiators $(\text{DMAT})_2\text{Ca}\cdot(\text{THF})_2$, $(\text{DMAT})_2\text{Sr}\cdot(\text{THF})_2$, and $(\text{DMAT})\text{Li}\cdot\text{TMEDA}$ showed no sign of reaction at room temperature. Polymerizations were only initiated after heating to ca. 60 °C (the Sr initiator showed the highest reactivity).

with SrI_2 . A crystal structure determination shows a monomeric complex with two additional THF ligands. Structural analyses of related Li, K, and Ca complexes reveal that the delocalization of the negative charge in the phenyl ring is metal dependent and decreases along the row $\text{K} > \text{Li} \geq \text{Sr} > \text{Ca}$. NMR analyses show exactly the same trend for the compounds in solution. The presented benzylstrontium complex contains two chiral benzylic centers and forms diastereomers. In apolar solvents both diastereomers are observed. Inversion of the chiral benzylic carbanion is fast at either higher temperatures or with extra added THF ligands. The process is concentration independent and follows a dissociative mechanism in which one of the $\text{Sr}-\text{C}_\alpha$ bonds is broken. The chiral benzylic carbon atom in the strontium complex shows faster inversion than that in the analogue benzylcalcium complex (Ca, 0.07 M, $\Delta G^\ddagger(T_{\text{coal}} 60^\circ\text{C}) = 16.8(3) \text{ kcal mol}^{-1}$; Sr, 0.08 M, $\Delta G^\ddagger(T_{\text{coal}} 30^\circ\text{C}) = 15.0(3) \text{ kcal mol}^{-1}$). The new benzylstrontium complex is an active initiator for the anionic living polymerization of styrene and is more reactive than its Ca analogue. This results in polymers with less tailing in the low molecular weight range and a narrower molecular weight distribution.

Experimental Section

General Comments. All experiments were carried out under argon using predried solvents and Schlenk techniques. The compound (DMAT)Li (**1**) was prepared according to the literature.¹⁷ Crystals of (DMAT)Li·TMEDA were obtained by dissolving the lithium compound with 2 equiv of TMEDA in warm hexane and subsequent cooling to -20°C . Crystals of (DMAT)K·THF were obtained by crystallization of the potassium compound from a benzene/THF mixture at 5°C . Crystal structures were dissolved with DIRDIF¹⁸ and refined with SHELXL-97.¹⁹ Geometry calculations and graphics were done with PLATON.²⁰

Synthesis of (DMAT)K (2**).** A solution of (DMAT)Li¹⁷ (2.08 g; 9.75 mmol) and potassium 2-methyl-2-pentanoate (1.50 g; 10.69 mmol) in diethyl ether (20 mL) was stirred for 10 min. The solvent was removed under vacuum, and the remaining yellow product was washed three times with 20 mL portions of hexane. Drying under vacuum yielded the solvent-free product in 83% yield (1.99 g). ¹H NMR (THF-*d*₈, 250 MHz, 20 °C): 0.37 (s, 9H, TMS); 1.92 (s, 1H, CH); 2.53 (s, 6H, NMe₂); 5.77 (t, 6.9 Hz, 1H, aryl); 6.67 (t, 7.0 Hz, 1H, aryl); 6.75–6.85 (m, 2H, aryl).

Synthesis of (DMAT)₂Ca·(THF)₂ (3**).** A mixture of 2-(dimethylamino)- α -trimethylsilylbenzylpotassium (3.81 g; 15.52 mmol) and CaI₂ (2.20 g; 7.49 mmol) in 20 mL of THF was stirred for 40 h. The mother liquor was isolated via centrifugation, and the remaining solid was extracted with 20 mL of benzene. Evaporation of the solvents from these combined extracts resulted in an orange-red sticky product, which was dissolved in a mixture of warm hexane (40 mL) and THF (15 mL). Cooling to -20°C yielded large light yellow crystals of (DMAT)₂Ca·(THF)₂ in 65% yield (2.75 g). ¹H NMR (toluene-*d*₈, 600 MHz, 20 °C): diastereomer A, 0.34 (s, 9H, TMS); 0.89 (s, 1H, CH); 1.25 (m, 8H, THF); 2.28 (very broad signal, 6H,

NMe₂); 3.19 (m, 8H, THF); 6.38 (t, 6.6 Hz, 1H, aryl); 6.72 (d, 7.8 Hz, 1H, aryl); 6.89 (d, 6.9 Hz, 1H, aryl); 7.12 (d, 7.8 Hz, 1H, aryl) and for diastereomer B, 0.45 (s, 9H, TMS); 1.24 (s, 1H, CH); 1.25 (m, 8H, THF); 2.42 (very broad signal, 6H, NMe₂); 3.19 (m, 8H, THF); 6.27 (t, 6.9 Hz, 1H, aryl); 6.55 (d, 7.8 Hz, 1H, aryl); 6.85 (d, 7.2 Hz, 1H, aryl); 7.18 (d, 7.8 Hz, 1H, aryl). ¹³C NMR (toluene-*d*₈, 600 MHz, 20 °C): diastereomer A, 2.8 (TMS); 25.3 (THF); 42.4 (NMe₂); 42.8 (CH); 68.3 (THF); 112.4, 119.2, 124.0, 126.3, 137.2 and 148.7 (ring) and for diastereomer B, 2.6 (TMS); 25.3 (THF); 45.0 (NMe₂); 47.1 (CH); 68.3 (THF); 112.4, 119.6, 123.8, 126.6, 136.8, and 147.8 (ring). ¹H NMR (THF-*d*₈, 250 MHz, 20 °C): 0.08 (s, 9H, TMS); 0.88 (br s, 1H, CH); 1.78 (m, 8H, THF); 2.49 (br s, 6H, NMe₂); 3.63 (m, 8H, THF); 6.18 (t, 7.0 Hz, 1H, ring); 6.67 (t, 7.0 Hz, 1H, ring); 6.75–6.85 (m, 2H, ring).

Synthesis of (DMAT)₂Sr·(THF)₂ (4**).** A mixture of 2-(dimethylamino)- α -trimethylsilylbenzylpotassium (1.44 g; 5.86 mmol) and SrI₂ (1.00 g; 2.93 mmol) in 30 mL of THF was stirred for 48 h. The reaction mixture was freed from solvent under high vacuum (0.01 Torr), and the remaining solid was extracted twice with 20 mL portions of benzene. Evaporation of the solvents from the combined orange benzene extracts resulted in an orange-red raw product, which was dissolved in a mixture of warm hexane (20 mL) and THF (10 mL). Cooling to -30°C yielded large yellow crystals of (DMAT)₂-Sr·(THF)₂ in 72% yield (1.36 g; 2.11 mmol). ¹H NMR (toluene-*d*₈, 600 MHz, 20 °C): diastereomer A, 0.40 (s, 9H, TMS); 1.04 (s, 1H, CH); 1.29 (m, 4H, THF); 2.26 + 2.35 (double singlet, 6H, NMe₂); 3.33 (m, 4H, THF); 6.32 (t, 7.0 Hz, 1H, aryl); 6.72 (d, 7.6 Hz, 1H, aryl); 6.89 (d, 7.2 Hz, 1H, aryl); 7.11 (d, 7.8 Hz, 1H, aryl) and for diastereomer B, 0.43 (s, 9H, TMS); 1.29 (s, 1H, CH); 1.29 (m, 4H, THF); 2.44 (very broad signal, 6H, NMe₂); 3.33 (m, 4H, THF); 6.25 (t, 7.1 Hz, 1H, aryl); 6.64 (d, 7.6 Hz, 1H, aryl); 6.84 (d, 7.3 Hz, 1H, aryl); 7.08 (d, 7.8 Hz, 1H, aryl). ¹³C NMR (toluene-*d*₈, 600 MHz, 20 °C): diastereomer A, 2.8 (TMS); 25.3 (THF); 42.6 (NMe₂); 47.0 (CH); 68.5 (THF); 110.8, 119.9, 123.2, 126.4, 135.6, and 148.3 (ring) and for diastereomer B, 2.9 (TMS); 25.3 (THF); 44.8 (NMe₂); 48.4 (CH); 68.5 (THF); 110.7, 119.9, 123.1, 126.4, 135.6, and 148.1 (ring). ¹H NMR (THF-*d*₈, 250 MHz, 20 °C): 0.08 (s, 9H, TMS); 0.88 (br s, 1H, CH); 1.78 (m, 4H, THF); 2.49 (br s, 6H, NMe₂); 3.63 (m, 4H, THF); 6.18 (t, 7.0 Hz, 1H, ring); 6.67 (t, 7.0 Hz, 1H, ring); 6.75–6.85 (m, 2H, ring).

Crystal structure data for (DMAT)Li·TMEDA (1**):** light yellow needles, monoclinic, $a = 9.800(5) \text{ \AA}$, $b = 15.486(4) \text{ \AA}$, $c = 16.348(7) \text{ \AA}$, $\beta = 119.02(3)^\circ$, $V = 2170(2) \text{ \AA}^3$, space group $P2_1/c$; formula (C₁₈H₃₆LiN₃Si), $M = 329.53$, $Z = 4$, $\rho_{\text{calcd}} = 1.009 \text{ g cm}^{-3}$, $\mu(\text{Mo K}\alpha) = 0.111 \text{ mm}^{-1}$; 4047 reflections were measured (Mo K α , graphite monochromator, $T = -90^\circ\text{C}$), 3813 independent reflections ($R_{\text{int}} = 0.011$), 2910 observed reflections with $I > 2.0\sigma(I)$. Solution by direct methods, full matrix least-squares refinement on F^2 to $R_1 = 0.068$, $wR_2 = 0.179$ and $S = 1.04$ (300 parameters). Non-hydrogens were refined anisotropically. Part of the TMEDA ligand shows large anisotropic displacement factors to a disorder generally observed in TMEDA ligands. The hydrogens have been partly taken from the difference Fourier map and were partly calculated. The benzylic hydrogens were observed and refined isotropically.

Crystal structure data for (DMAT)K·THF (2**):** orange blocks, monoclinic, $a = 9.954(1) \text{ \AA}$, $b = 11.893(1) \text{ \AA}$, $c = 17.448(2) \text{ \AA}$, $\beta = 114.616(8)^\circ$, $V = 1877.8(3) \text{ \AA}^3$, space group $P2_1/c$; formula (C₁₆H₂₈KNOSi), $M = 317.58$, $Z = 4$, $\rho_{\text{calcd}} = 1.123 \text{ g cm}^{-3}$, $\mu(\text{Mo K}\alpha) = 0.344 \text{ mm}^{-1}$; 4254 reflections were measured (Mo K α , graphite monochromator, $T = -90^\circ\text{C}$), 4111 independent reflections ($R_{\text{int}} = 0.021$), 2664 observed reflections with $I > 2.0\sigma(I)$. Solution by direct methods, full matrix least-squares refinement on F^2 to $R_1 = 0.059$, $wR_2 = 0.170$ and $S = 1.02$ (261 parameters). Non-hydrogens were refined anisotropically. Part of the hydrogens have been taken from the

(17) Jastrzebski, J. T. B. H.; van Koten, G.; Knaap, C. T.; Schreurs, A. M. M.; Kroon, J.; Spek, A. L. *Organometallics* **1986**, *5*, 1551.

(18) Beurskens, P. T.; Admiraal, G.; Beurskens, G.; Bosman, W. P.; de Gelder, R.; Israel, R. *The DIRDIF Program System*; Crystallography Laboratory, University of Nijmegen: The Netherlands, 1994.

(19) Sheldrick, G. M. *SHELXL-97, Programs for the Determination of Crystal Structures*; Universität Göttingen: Germany, 1997.

(20) Spek, A. L. *PLATON, A Multipurpose Crystallographic Tool*; Utrecht University: Utrecht, The Netherlands, 2000.

difference Fourier map and part were calculated. The benzylic hydrogens were observed and refined isotropically.

Crystal structure data for [(DMAT)₂Sr·(THF)₂][THF] (4): yellow blocks, triclinic, $a = 10.0146(5)$ Å, $b = 10.3125(5)$ Å, $c = 20.208(1)$ Å, $\alpha = 94.710(5)^\circ$, $\beta = 89.994(5)^\circ$, $\gamma = 105.122(4)^\circ$, $V = 2007.4(2)$ Å³, space group $P\bar{1}$; formula (C₃₂H₅₆N₂O₂·Si₂Sr)·(C₄H₈O), $M = 716.69$, $Z = 2$, $\rho_{\text{calcd}} = 1.186$ g cm⁻³, $\mu(\text{Mo K}\alpha) = 1.436$ mm⁻¹; 9311 reflections were measured (Mo K α , graphite monochromator, $T = -90$ °C), 8809 independent reflections ($R_{\text{int}} = 0.009$), 7769 observed reflections with $I > 2.0\sigma(I)$. Absorption correction with ABSPSI incorporated in the program PLATON.¹⁹ Solution by direct methods, full matrix least-squares refinement on F^2 to $R_1 = 0.036$, $wR_2 = 0.099$ and $S = 1.05$ (459 parameters). Non-hydrogens were refined anisotropically. Hydrogens were calculated and were refined isotropically riding on their pivot atom. The benzylic hydrogens were found in a difference Fourier map and were refined isotropically with free displacement factors.

Polymerization Experiments. Polymerizations of styrene were performed in a thermostated 100 mL stainless steel reactor at normal pressure and a temperature of 50 °C. In a typical polymerization experiment the reactor was loaded with 90 mL of dry cyclohexane and 11.5 mL (ca. 100 mmol) of freshly distilled (from alox-perls) styrene. A solution of the initiator in 1.0 mL of benzene/cyclohexane (0.1 mmol for RLi and 0.05 mmol for the dibenzyl alkaline-earth metal complexes) was added via a port. The usual appearance of a red color indicated that the polymerization started immediately.

After a polymerization time of 30 min the mixture was quenched with oxygen-free methanol. Evaporation of all solvents yields the polymer in quantitative yields.

Polymer analyses were carried out by GPC and high-temperature ¹H and ¹³C NMR (solvent tetrachloroethane-*d*₂). The molecular weights usually showed a Gaussian distribution around 100.000 Da (expected on basis of the monomer/initiator ratio). The tacticity of the polymer was checked by analyzing the ¹³C NMR signal for the C_{ipso} phenyl ring carbon. Isotactic or syndiotactic arrangements would give singlets at 146.1 and 145.5 ppm, respectively. All our samples show broad multiplet structures between 145.2 and 146.6 ppm.

Acknowledgment. We are grateful to the BASF AG (Ludwigshafen, Germany) for financing this project and for the GPC analyses of the polymers. Prof. Dr. H.-H. Brintzinger (Konstanz) and Dr. K. Knoll (Ludwigshafen) are kindly acknowledged for helpful discussions. Mrs. A. Friemel is thanked for measuring 600 MHz spectra.

Supporting Information Available: Atomic fractional coordinates, bond distances and angles, hydrogen atom positions, and anisotropic thermal parameters for the complexes **1**, **2**, and **4** are available free of charge via the Internet at <http://pubs.acs.org>.

OM010444J